

PDF hosted at the Radboud Repository of the Radboud University Nijmegen

The following full text is a publisher's version.

For additional information about this publication click this link.

<http://hdl.handle.net/2066/22259>

Please be advised that this information was generated on 2017-12-05 and may be subject to change.

Immunohistochemical analysis of unsutured and sutured corneal wound healing

Gerrit R. J. Melles, Nirmala SundarRaj¹, Perry S. Binder², Marcel M. van der Weiden³, Robert H. J. Wijdh⁴, W. Houdijn Beekhuis⁴ and Janet A. Anderson²

Department of Ophthalmology, University of Nijmegen, The Netherlands, ¹University of Pittsburgh School of Medicine, Pittsburgh, ²National Vision Research Institute, San Diego, USA, ³Department of Pathological Anatomy and ⁴Eye Hospital, Erasmus University, Rotterdam, The Netherlands

Abstract

In the unsutured partial thickness penetrating wounds of the cornea, the epithelium migrates over the wounded stromal surface prior to the onset of stromal regeneration. To determine the possible effects of the epithelial ingrowth on the organization of the stromal scar tissues, the healing of unsutured and sutured wounds was compared immunohistochemically. Immunostaining patterns for fibronectin, types III, VI and VII collagen, keratan sulfate proteoglycan (KSPG), and intermediate filament-associated protein (IFAP 130) in fibroblasts, were analyzed in unsutured and adjacent sutured keratotomy wounds in monkeys, at 2–9 weeks after surgery. At 2–4 weeks, fibronectin, type III and type VI collagen showed a lamellar interweaving pattern across unsutured wounds that was absent in sutured wounds. Type VII collagen was detected along the entire depth of regenerated stroma in unsutured wounds, but not in sutured wounds indicating that the epithelium had formerly been present in the regenerated stroma in unsutured wounds. Fibroblasts in both types of wounds expressed IFAP 130, but staining was more pronounced in sutured wounds. At 5–9 weeks, cellular re-activation, as judged from the expression for IFAP 130, was concomitant with a loss of lamellar interweaving with fibronectin, type III and type VI collagen across unsutured wounds, and proceeded in a posterior to anterior direction. In contrast, in sutured wounds, lamellar interweaving was established in anterior to posterior direction. At all postoperative times, unsutured and sutured wounds showed minimal staining for KSPG in the anterior scar. The distribution patterns of fibronectin, type III and type VI collagen and IFAP 130 suggested that unsutured wounds obtain a more advanced wound repair compared to sutured wounds during the early stages of healing which is followed by ineffective wound remodeling from the posterior to anterior

regions. In sutured wounds, effective wound repair may be established from the anterior to posterior regions, after a relatively long period of a disorganized state of the scar tissues. These observations suggest that the temporary presence of an epithelial plug within an unsutured wound and/or wound gaping induce a different stromal healing response from that in the sutured wounds, that results in an eventual ineffective wound repair. *Curr. Eye Res.* 14: 809–817, 1995.

Key words: cornea; wound healing; collagen; glycosaminoglycan; radial keratotomy; immunohistochemistry; monkey

Introduction

Clinical and laboratory studies of corneal wounds (1, 2, 3) have shown incomplete healing of unsutured wounds, whereas sutured wounds appear to regain lamellar continuity over time. This finding suggests that lack of wound apposition and concomitant epithelial ingrowth in the early phases of the healing of unsutured wound, modifies the stromal healing response (1, 2, 3). To what extent stromal repair is altered by the presence of an epithelial plug and/or wound gaping may be elucidated by comparing healing of unsutured with that of sutured wounds.

After wounding, fibronectin originating from the tear film (4) binds to the exposed stromal surface(s) and cell membranes, to provide a temporary scaffolding for epithelial migration and adhesion, prior to formation of a basement membrane over the wound edges (5, 6, 7, 8, 9, 10). In later phases of healing, fibronectin may be produced by fibroblasts (7, 10), and the fibronectin matrix may modulate scar tissue organization (10, 11, 12, 13). Fibronectin within the wound may therefore reflect the interaction of both epithelial and stromal cells with their surrounding matrix.

Keratan sulfate proteoglycan (KSPG) may have a role in corneal transparency and hydration, by its water binding and

Correspondence: N. SundarRaj, Department of Ophthalmology, University of Pittsburgh School of Medicine, 203 Lothrop Street, Eye and Ear Institute, Pittsburgh, PA 15213, USA

collagen spacing properties (14). In early phases of healing, a reduced level and/or a less sulfated type of KSPG (15), and an increase of highly sulfated chondroitin sulfate, may be concurrent with opacification and excess hydration of the scar. In later phases of healing, near normal levels of KSPG may be concurrent with restoration of transparency and normal hydration (14, 16, 17). The distribution of KSPG may therefore reflect the degree of wound restoration, and may add to our understanding of how the extracellular matrix is organized within the scar.

Although conflicting reports have described its presence or absence in the adult corneal stroma (6, 18, 19, 20, 21, 22), type III collagen may be present in the fetal and regenerating cornea (23, 24, 25). By its interaction with fibronectin and type I collagen, type III collagen may have a role in controlling early fibrillogenesis (20, 26). The expression of type III collagen may therefore suggest recapitulation of fetal developmental stages of collagen fibrillogenesis.

Type VI collagen is present as a fine filamentous network in between type I collagen fibers where it may provide mechanical stability by restricting lateral displacement of the fibers (27, 28, 29, 30, 31). Because proteoglycans are bound to type VI collagen, it may also have a role in corneal transparency (27, 31). In corneal wounds, type VI collagen may be a measure for the regeneration of lamellar continuity across the wound (29).

As the main component of anchoring fibrils, the appearance of type VII collagen indicates the presence of epithelial-substratum adhesion sites (32, 33). Since type VII collagen is synthesized by epithelial cells (34, 35), the localization of this collagen may indicate where the epithelium previously interacted with the stroma in unsutured wounds (3, 5, 6). If so, type VII collagen may show where the epithelium was formerly present in the regenerated tissue.

Intermediate filaments may be involved in cellular and cell-matrix interactions during corneal development and wounding (36). Following wounding, fibroblasts express an intermediate filament-associated protein (IFAP 130) (36), that is not detected in quiescent cells. IFAP 130 may therefore be used to identify activated fibroblasts, and to compare the duration of their activated condition in healing wounds (5, 6).

To determine how the former presence of an epithelial plug affects the stromal healing response, unsutured and sutured keratotomy wounds were analyzed by immunolabeling for fibronectin, type III, type VI and type VII collagen, KS and IFAP 130.

Materials and methods

Radial keratotomy (RK) procedures were performed by one of us (GM), in seven male monkeys (*Macaca mulatta*), 5–7 kg in weight, aged 7–8 years. All animals were housed and treated according to the Association for Research in Vision and Ophthalmology resolution for animal care.

Each monkey was anaesthetized with ketamine-HCl [Ketamine 100 mg/ml, Tesink Veterinary Products, Oudewater, The Netherlands (NL)] and acepromazine (Vetaranquil 10 mg/ml,

Sanory, Maassluis, NL). A double edged diamond blade (Drukker International, Amsterdam, NL) was set to achieve 90% of the thinnest ultrasonic central corneal reading, to avoid corneal perforation (Humphrey ultrasonic pachometer, model 850, Humphrey, San Leandro, CA). Blade extension was measured monocularly under the operating microscope (Zeiss, Weesp, NL) at maximum magnification using a coin gauge. After marking a 3.0 mm optical clear zone (OCZ) centered on the pupil (Moria Instruments, Paris, France), centripetal incisions were made using the perpendicular cut edge, with the eye stabilized with a toothed forceps at the opposite limbus.

All monkeys underwent a bilateral, six incision RK procedure; three semi-radial incisions were placed in each half of the cornea (1). Incisions at 1:30, and 7:30 o'clock in the right eye, at 4:30, and 10:30 o'clock in the left eye were sutured with two interrupted 10-0 nylon sutures on a four wire needle (Alcon monofilament Nylon, Gorinchem, NL).

Monkeys were terminated using an overdose of intravenous pentobarbital-Na (Euthesate 200 mg/ml, APharma, Arnhem, NL), the eyes were enucleated, and sutures were removed from tissue designated for cryostat sectioning. Corneo-scleral rims with a suture identifying the 12 o'clock meridian of the scleral flap, were obtained by incising the sclera for 360° anterior to the equator leaving a 3 mm scleral rim, and gently removing the anterior uveal tissue. With a razor blade knife, corneas were cut in half perpendicularly to the incisions at 1:30, and 7:30 o'clock in the right eye, to those at 4:30, and 10:30 o'clock in the left eye (Fig. 1).

The inferior-temporal corneal half from the right eye, and the superior-nasal half from the left eye intended for histochemical analysis (Fig. 1) were stored frozen at -70°C . Cryostat sections (5–6 μm), obtained at six different portions of the incisions, were transferred to glass slides and immunoreacted with specific antibodies at appropriate dilutions using an indirect fluorescein isothiocyanate (FITC)-conjugated antibody technique (6). Tissue sections on the slides were reacted successively with 5% heat-inactivated rabbit serum in phosphate-buffered saline for 45 min, the appropriate antibody (10

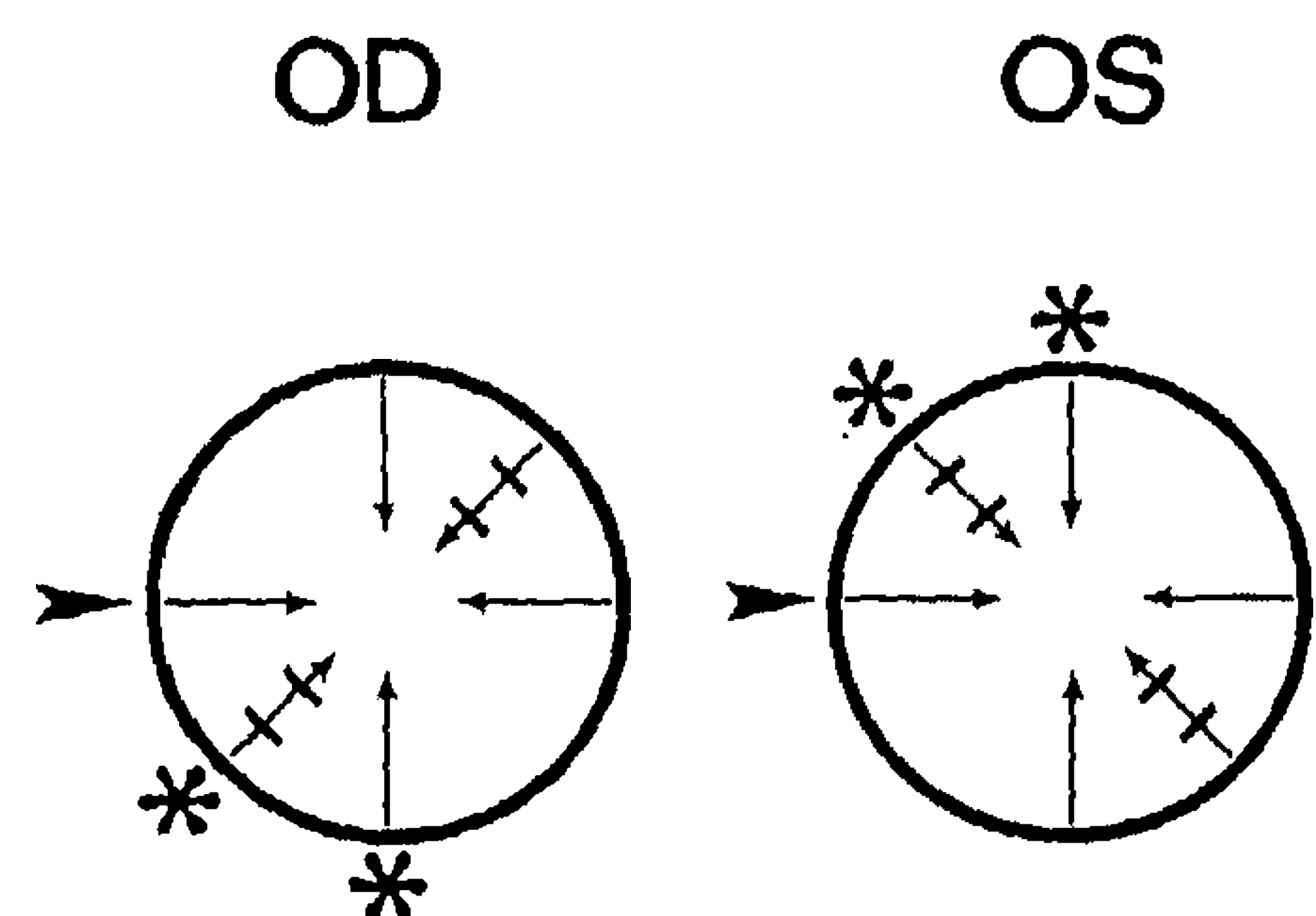


Figure 1. Keratotomy and suture patterns performed in 14 monkey corneas. The inferior-temporal corneal half from the right eyes, and the superior-nasal half from the left eyes were frozen for immunostaining. Astericks indicate the unsutured and sutured wounds evaluated by immunostaining; arrowheads show the incisions that were reopened and sutured wounds (not included in this study).

$\mu\text{g/ml}$) in 5% heat-inactivated rabbit serum for 45 min, and FITC-conjugated rabbit antimouse IgG (preabsorbed with human corneal tissue) at a 1:20 dilution in 5% heat-inactivated rabbit serum for 45 min. The sections were washed three times with phosphate-buffered saline between each of the above treatments. Preabsorption of the FITC-conjugated second antibody was performed by incubating the antibody with the insoluble fraction of a homogenate of pulverized corneal tissue, at 4°C for 24 h. After centrifugation at 10,000 g for 30 min, the supernatant was used for immunostaining. This

preabsorption reduced the non-specific binding of FITC to the tissue. The stained sections were mounted in glycerin-gelatin and examined and photographed with a photomicroscope (Vanox, Olympus Optical Co Ltd, Tokyo, Japan) with fluorescence attachments and epifluorescence objectives. Staining patterns were evaluated by three of the authors (GM, NS, MW).

Two unsutured and two sutured wounds in the frozen halves from both eyes of the same animal (Fig. 1) were evaluated for each postoperative time interval, i.e. one animal was terminated at 2, 3, 4, 5, 6, 7 and 9 weeks after the primary surgery. The

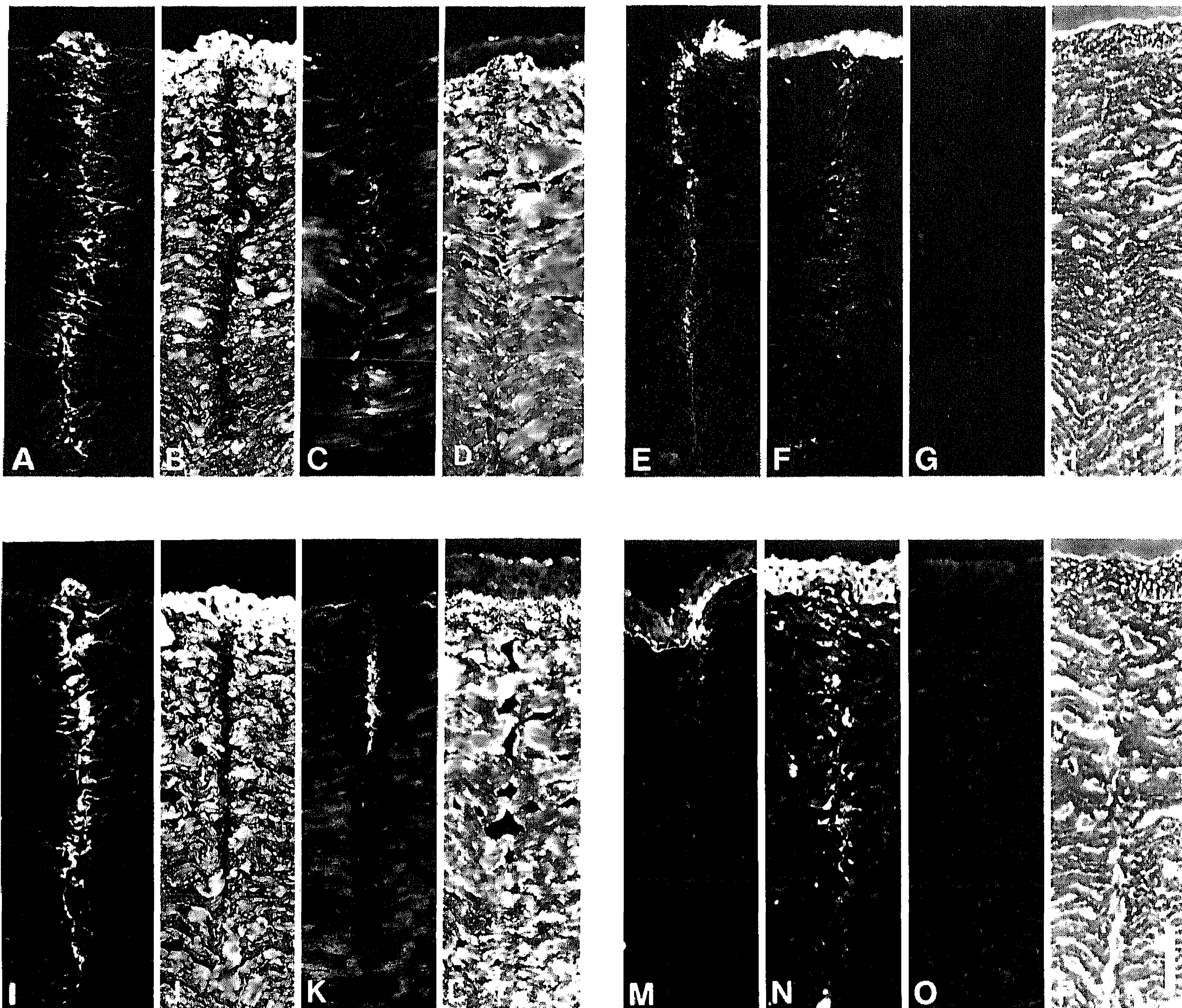


Figure 2. Immunofluorescence staining of an unsutured (A–H) and a sutured (I–P) wound, 3 weeks postoperative: fibronectin (A and I), KSPG (B and J), type III collagen (C and K), type VI collagen (D and L), type VII collagen (E and M), IFAP 130 (F and N), negative control (G and O), and phase contrast photomicrographs for histologic orientation (H and P). Note that fibrillar-like interweaving with fibronectin, type III and type VI collagen in unsutured wounds is associated with apparent tissue continuity in phase contrast images. Compare to Figures 3 and 4 (Bar = 100 μm).

following antibodies were used: (1) antifibronectin (polyclonal, CLB, Amsterdam, NL), (2) antikeratan sulfate monoclonal antibody J10 (5, 6, 37), (3) antitype III collagen monoclonal antibody 715, directed against the bacterial collagenase-resistant region of type III collagen (6, 38), (4) antitype VI collagen (Telios Pharmaceuticals, Inc., San Diego, CA), (5) antitype VII collagen (34, 39), (Antitype VII collagen was a gift from J. C. R. Jones, PhD, Northwestern University, Chicago, IL), and (6) antibody M12, directed against intermediate filament-associated protein (IFAP130) (5, 6, 36).

Results

A total of 14 unsutured and 14 sutured wounds (Fig. 1) was evaluated after immunolabeling for fibronectin, KSPG, type III, type VI and type VII collagen, and fibroblast intermediate filament-associated protein (IFAP 130), at weekly intervals from 2 to 9 weeks after surgery (Figs. 2 to 4). Staining patterns in sutured and unsutured wounds appeared to be comparable among mate eyes; no differences in staining were found between wounds in the inferior-temporal corneal half of the

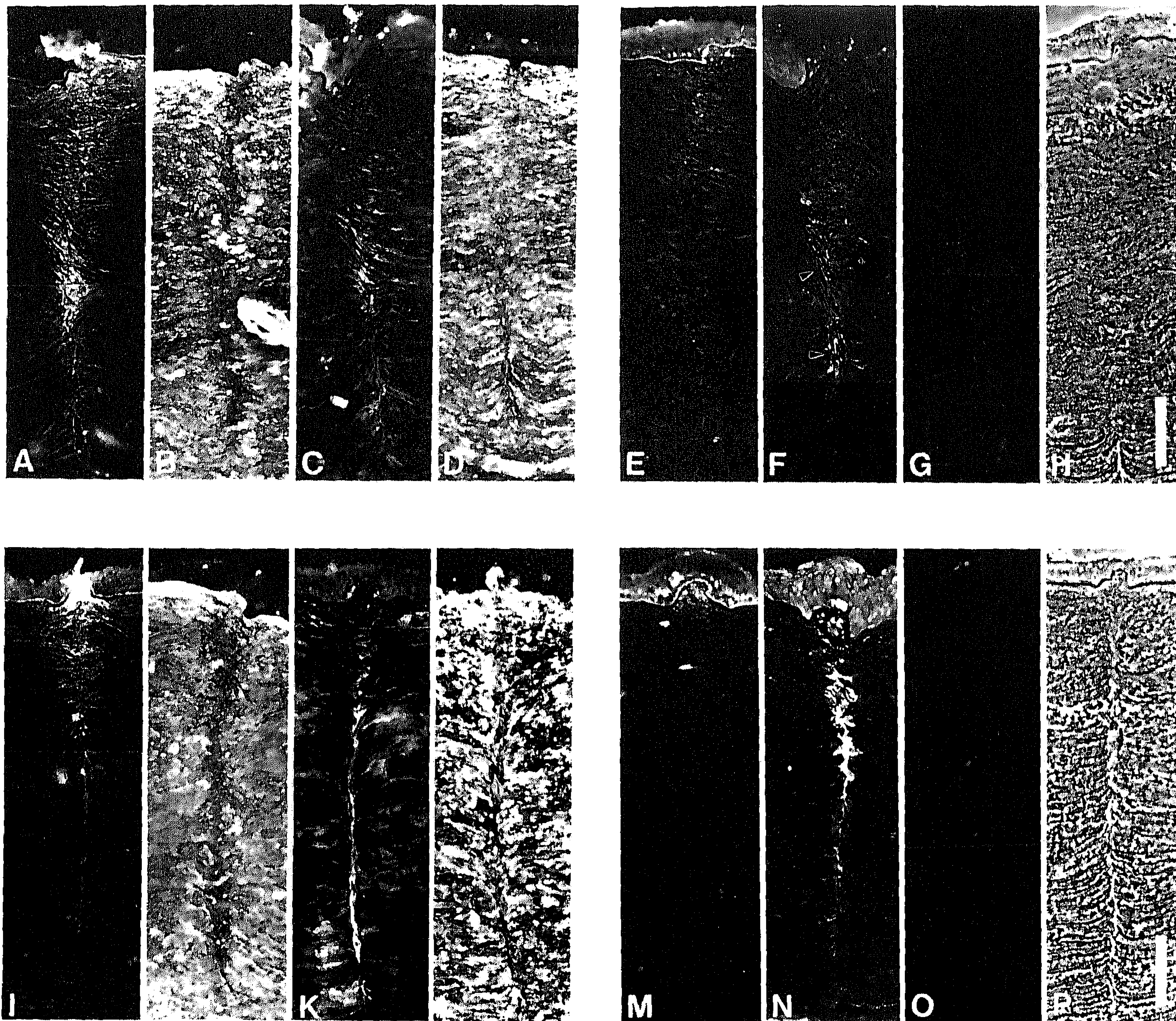


Figure 3. Immunofluorescence staining of an unsutured (A-H) and a sutured (I-P) wound, 6 weeks postoperative: fibronectin (A and I), KSPG (B and J), type III collagen (C and K), type VI collagen (D and L), type VII collagen (E and M), IFAP 130 (F and N), negative control (G and O), and phase contrast photomicrographs for histologic orientation (H and P). Note that the posterior, unsutured wound shows less, and the anterior, sutured wound more scar tissue organization perpendicular to the wound, as compared to similar types of wounds at 3 weeks. The area indicated by the arrowheads in 'd' is shown at a higher magnification in Figure 5 (Bar = 100 μ m).

right eye, and the superior-nasal half of the left eye (Fig. 1). Possible pulling effects the sutures may cause on the adjacent unsutured wounds were taken into account while drawing the conclusions on the healing of unsutured wounds.

Two, three and four weeks

Brilliant staining for fibronectin was present over the full depth of both types of wounds, in a 'V'-shaped pattern (Figs. 2A and 2I). In unsutured wounds, a dense, fibrillar-like fluorescence was seen across the entire wound; lamellae of opposing wound edges appeared to interweave (Fig. 2A). In sutured wounds, lamellar interweaving was absent; fibronectin was

lining the opposing stromal wound edges and the scar was seen as a discontinuous stromal lamellae (Fig. 2I).

A diffuse staining for KSPG was seen throughout the unwounded stroma. Unsutured and sutured wounds were seen as dark areas with minimal staining in between the anterior wound edges; no differences in staining patterns were found between both types of wounds (Figs. 2B and 2J).

Staining for type III collagen showed a sparse fluorescence across unsutured wounds (Fig. 2C). In contrast, sutured wounds had a distinct, mottled fluorescence along the wound edges in the anterior and mid regions (Fig. 2K). A band of non-fluorescent stroma directly adjacent to the wound, contrasted with diffuse staining in the unwounded stroma.

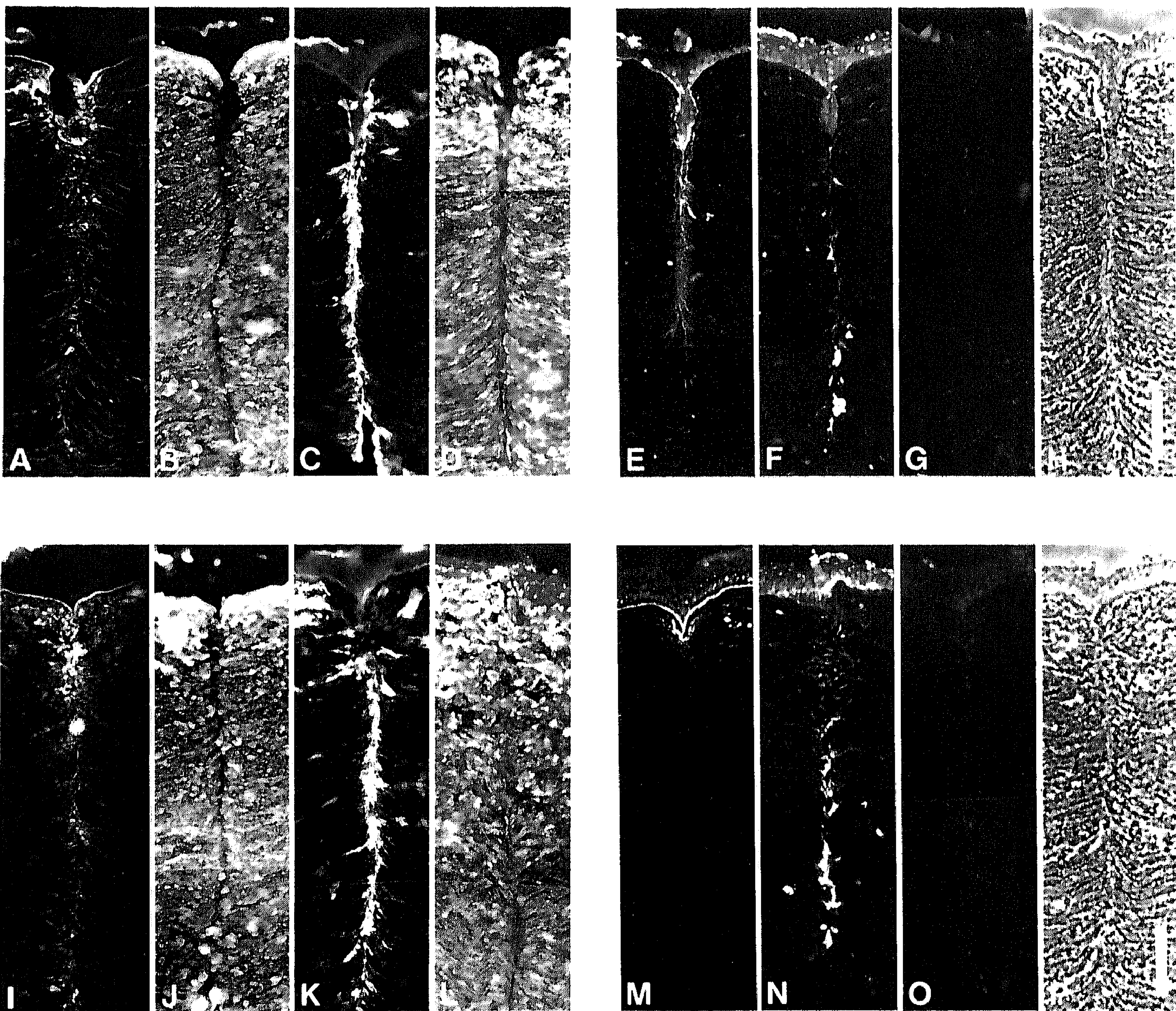


Figure 4. Immunofluorescence staining of an unsutured (A-H) and a sutured (I-P) wound, 9 weeks postoperative: fibronectin (A and I), KSPG (B and J), type III collagen (C and K), type VI collagen (D and L), type VII collagen (E and M), IFAP 130 (F and N), negative control (G and O), and phase contrast photomicrographs for histologic orientation (H and P). (Bar = 100 µm).

Type VI collagen showed a very fine, packed, fibrillar-like staining throughout the unwounded stroma. Unsutured wounds could hardly be identified, since the fibrillar-like staining pattern for type VI collagen was continuous across the wounds (Fig. 2D). In contrast, sutured wounds exhibited a discontinuity of staining; no fluorescence for type VI collagen was present between the wound edges (Fig. 2L).

A band of fine punctate staining for type VII collagen was seen over the entire scar of unsutured wounds (Fig. 2E). This band gradually decreased in width and density toward the posterior wound. In sutured wounds, punctate fluorescence was restricted to the wound top region (Fig. 2M).

Fibroblasts reacted with IFAP 130 over the entire depth of both types of wounds in a 'V'-shaped pattern (Figs. 2F and 2N). Staining was more intense in sutured wounds; fluorescence in unsutured wounds diminished to negligible levels three to four weeks after surgery.

Five and six weeks

In unsutured wounds, a fibrillar-like staining pattern for fibronectin was seen in the anterior and mid regions, whereas a loss of lamellar interweaving with fibronectin was seen in the posterior wound region (Fig. 3A). In sutured wounds, fibrillar-like staining was present across the anterior wound, but the mid and posterior wound regions still displayed lamellar discontinuity with fibronectin lining the wound edges (Fig. 3I).

Staining patterns for KSPG appeared to be similar to those at two to four weeks (Figs. 3B and 3J). Unsutured wounds showed a sparse fluorescence for type III collagen that was more intense in the mid and posterior regions (Fig. 3C). Sutured wounds had a sparse, lamellar fluorescence across the wound top region, but showed a linear staining along the mid and posterior wound edges (Fig. 3K).

Unsutured wounds showed a fibrillar-like fluorescence for type VI collagen across the anterior and mid regions, that was absent in between the posterior wound edges (Fig. 3D). Sutured wounds showed a fibrillar-like staining pattern across the anterior region, but absence of staining in the mid and posterior regions (Fig. 3L).

Staining patterns for type VII collagen in both types of wounds appeared to be similar to those at two weeks, although the punctate staining in unsutured wounds had a more scattered appearance at later postoperative times (Figs. 3E and 3M).

Expression of IFAP 130, that had gradually diminished in fibroblasts with an orientation perpendicular to the wound edges in unsutured wounds, re-appeared in posterior fibroblasts that showed an apparent re-orientation parallel to these wounds (Figs. 3F and 5). Fibroblasts in sutured wounds still showed intense staining for IFAP 130 in the mid and posterior regions (Fig. 3N).

Seven and nine weeks

Staining for fibronectin had diminished in both types of wounds (Figs. 4A and 4I). In unsutured wounds, fibrillar-like staining for fibronectin across the wound was restricted to anterior region (Fig. 4A). Sutured wounds showed fibrillar staining in the anterior and mid regions (Fig. 4I).

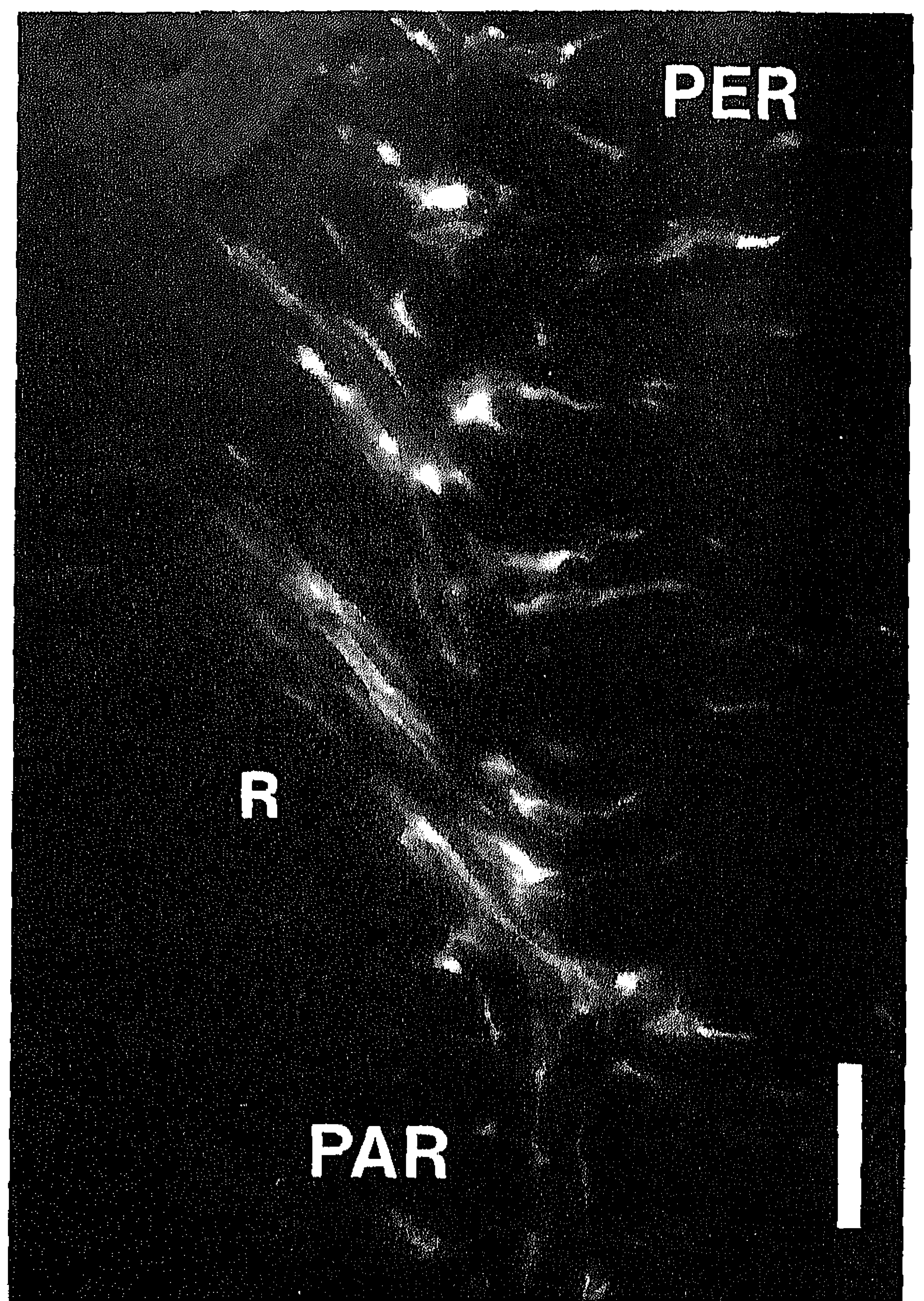


Figure 5. Immunofluorescence staining of the mid-posterior region of an unsutured wound, 6 weeks postoperative. Posterior fibroblasts, that appear to reorient (R) from a perpendicular (PER) to a parallel (PAR) orientation to the wound, show positive staining for IFAP 130. This may suggest re-activation of these fibroblasts, since the cells were found to be quiescent at 3 to 4 weeks after surgery (Bar = 10 μ m).

Staining patterns for KSPG were similar to those found at earlier time intervals (Figs. 4B and 4J). Both types of wounds showed a pronounced staining for type III collagen lining the wound edges, with a feathered appearance (Figs. 4C and 4K). Unsutured wounds showed discontinuity of staining for type VI collagen over the entire wound depth (Fig. 4D), whereas a continuous fibrillar-like staining pattern was seen across anterior regions of the sutured wounds (Fig. 4L).

After nine weeks, only a dispersed punctate pattern for type VII collagen was present in the anterior and mid regions of unsutured wounds (Fig. 4E). In both types of wounds IFAP 130 was detectable in the mid and posterior regions (Figs. 4F and 4N).

Discussion

A previous study (5), examining keratotomy wound healing in rabbits using immunohistochemical markers, has described the process of epithelial plug elimination, with repetitive

formation of a basement membrane onto newly deposited scar tissue. A return of fibroblasts to a quiescent state coincided with the formation of a continuous basement membrane and reduced extracellular matrix (ECM) synthesis. In perforating wounds, synthesis of type III collagen was restricted to the posterior wound (23), and that of type VI collagen to the anterior and mid wound (27). In keratotomy wounds in cats, the orientation of fibrillar fibronectin correlated with that of myofibroblasts, and therefore with the hypothetical direction of wound contraction (10, 12, 13, 40).

In the current study, immunostaining of unsutured wounds was compared with that of sutured wounds, to reveal how the former presence of ectopic epithelium within the stroma contributes to unsutured wound healing. Fibronectin was used to identify the presence of a protein matrix that may mediate binding of epithelial cells and fibroblasts to the ECM (6, 7, 8, 9, 10, 11, 12, 13). KSPG and type III collagen were used to determine the maturity of the scar (23). Type VI collagen was used to determine the recovery of lamellar continuity across the wound (27, 29). Type VII collagen was chosen to localize epithelial attachment sites (6, 32, 34, 35). Fibroblast intermediate filament-associated protein (IFAP 130) was used to monitor fibroblast activation during healing (5, 6, 36).

In unsutured and sutured wounds, staining for KSPG was less intense than in the surrounding, unwounded stroma. This may agree with the lower than normal concentration of KSPG in nonperforating (17) and perforating (16, 41) unsutured wounds in rabbits. In the latter wounds, KSPG synthesis was restricted to the anterior wound at two weeks, and to the anterior and mid wound at eight weeks after surgery. In our study, minimal KSPG deposition appeared to be restricted to the anterior regions of unsutured and sutured wounds, at all postoperative time intervals. The reduced levels of KSPG have been suggested to result from different oxygenation levels in scar compared to normal tissue (15, 42) or from inability to detect the altered, less sulfated KSPG molecule (15). Hence, the weak staining for KSPG in both unsutured and sutured wounds suggests that KSPG synthesis is incomplete in the first months after surgery, in both types of wounds.

Unsutured wounds showed type VII collagen deposition over the full depth of the wound, whereas it was present only in the top region of sutured wounds. Assuming that type VII collagen is of epithelial origin and synthesized at the epithelial-stromal interface (5, 6, 32, 34, 35), its presence within the scar not only suggests the former presence of epithelium within these wounds (5, 6) but points to the fact that the epithelium was actively laying down type VII collagen during continuous remodeling of the tissues. Since type VII collagen is synthesized during (35) or after (34) formation of hemidesmosomes and a basement membrane, our observations suggest that an epithelial adhesion complex is laid down after epithelial ingrowth in unsutured wounds, and that anchoring fibrils or their remnants remain temporarily within the scar after elimination of the epithelial plug.

Since expression of IFAP 130 by fibroblasts reflects cellular activation (36), a gradual decrease in IFAP 130 over the depth of unsutured wounds indicates that fibroblastic activity was

higher toward the anterior wound region. This agrees with a progression in healing from the bottom to the top of the incision with concurrent elimination of the epithelial plug, and more scar tissue deposition in the anterior than in the posterior wound (1). However, this hypothesis does not explain a similar 'V'-shaped distribution for IFAP 130 over the depth of sutured wounds, in which healing may be expected to start simultaneously at all stromal regions. These findings suggest that fibroblast activation differs among healing stromal regions, irrespective of the former presence of an epithelial plug.

The distribution patterns of fibronectin, type III and type VI collagen suggested a different scar tissue organization in unsutured compared to sutured wounds, and a change in organization in each type of wound over time. In early phases of healing, unsutured wounds showed a fibrillar interweaving with fibronectin, type III and type VI collagen across the entire wound. In contrast, the discontinuous staining pattern across the sutured wounds were seen as a stromal disruption. Fibronectin and type III collagen were deposited along the wound edges and type VI collagen was absent from the wounds. The distribution patterns of these ECM molecules may therefore indicate that unsutured wounds approximate anatomical repair at early postoperative time intervals, compared to incomplete repair in sutured wounds. Although the unsutured wounds may have been subjected to some additional wound gape due to retraction from sutures in adjacent wounds, this may not explain the better early repair of the unsutured wounds.

In later phases of healing, a loss of fibrillar interweaving with fibronectin, type III and type VI collagen was seen in the posterior regions of unsutured wounds. In contrast, sutured wounds showed the establishment of fibrillar interweaving with fibronectin, type III and type VI collagen across the anterior wound regions. Therefore, the change in ECM distribution over time suggests a loss of the initial near normal anatomical organization of the ECM in unsutured wounds, from the posterior to anterior regions; and an approximation toward normal ECM distribution in sutured wounds progressing from the anterior to posterior regions.

These changes in ECM distribution appeared to be closely related to the patterns of fibroblast orientation observed in the complementary corneal halves, that were evaluated with light and transmission electron microscopy (43). In unsutured wounds, an initial fibroblast orientation perpendicular to the wound (edges) was followed by a re-orientation of posterior fibroblasts parallel to the wound. During cell re-orientation, the cells appeared to become re-activated (Fig. 5), after they had obtained a quiescent appearance as early as three weeks after surgery. In sutured wounds, fibroblasts with an overall orientation parallel to the wound, showed a highly activated condition up to nine weeks after surgery. In late phases of healing, the cells in the anterior and mid regions showed less activation and an orientation perpendicular to the wound. Since fibroblast orientation reflected ultrastructural collagen fiber orientation (44), the re-orientation of the cells resulted in a progressive loss of collagen fiber continuity across unsutured wounds, and the establishment of fiber continuity in sutured wounds (unpublished data).

Therefore, the distribution patterns of fibronectin, type III and type VI collagen and IFAP 130, as well as the biphasic patterns of fibroblast orientation, suggest that healing in unsutured and sutured wounds varies over wound depth, and that it is established in opposite directions. Sutured wounds may initially heal more slowly, but obtain lamellar continuity over time. In contrast, early near normal anatomical repair and subsequent ineffective remodeling characterized the healing of unsutured wounds, which may, in part, have resulted from early epithelial ingrowth.

Acknowledgements

We gratefully thank C. M. Mooy, MD; J. B. H. J. van Lier, BS; J. C. R. Jones, PhD; H. D. Wiersema; P. M. C. A. van Eerd, DVM.; W. M. Klapwijk (T.N.O. primate center, Delft, The Netherlands); and H. A. W. Bongaarts for their valuable advice and cooperation.

Supported by grants from: the Department of Ophthalmology, University of Nijmegen, The Netherlands; the Flieringa Foundation and the Store Foundation, Rotterdam, The Netherlands; NIH EY03263 (Dr SundarRaj) and EY08098; and the National Vision Research Institute, San Diego, USA.

References

- Binder, P. S. (1989) What we have learned about corneal wound healing from refractive surgery. *Refract. Corneal Surg.* **5**, 98–120.
- Binder, P. S., Wickham, M. G., Zavala, E. Y. and Akers, P. H. (1980) Corneal anatomy and wound healing. In: *Trans New Orleans Acad. Ophthalmol.* Pp. 1–35. CV Mosby Co. St Louis.
- Melles, G. R. J. and Binder, P. S. (1990) A comparison of wound healing in sutured and unsutured corneal wounds. *Arch. Ophthalmol.* **108**, 1460–1469.
- Jensen, O. L., Glud, B. S. and Eriksen, H. O. (1985) Fibronectin in tears following surgical trauma to the eye. *Acta Ophthalmol.* **63**, 346–350.
- Goodman, W. M., SundarRaj, N., Garone, M. Arffa, R. C. and Thoft, R. A. (1989) Unique parameters in the healing of linear partial thickness penetrating corneal incisions in rabbit: immunohistochemical evaluation. *Curr. Eye Res.* **8**, 305–316.
- SundarRaj, N., Geiss, M. J., Fantes, F., Hanna, K., Anderson, S. C., Thompson, K. P., Thoft, R. A. and Waring, G. O. (1990) Healing of excimer laser ablated monkey corneas. An immunohistochemical evaluation. *Arch. Ophthalmol.* **108**, 1604–1610.
- Phan, T. M., Foster, C. S., Zagachin, L. M. and Colvin, R. B. (1989) Role of fibronectin in the healing of superficial keratectomies *in vitro*. *Invest. Ophthalmol. Vis. Sci.* **30**, 386–391.
- Zieske, J. D., Higashijima, S. C., Spurr-Michaud, S. J. and Gipson, I. K. (1987) Biosynthetic responses of the rabbit cornea to a keratectomy wound. *Invest. Ophthalmol. Vis. Sci.* **28**, 1668–1677.
- Fujikawa, L. S., Foster, C. S., Gipson, I. K. and Colvin, R. B. (1984) Basement membrane components in healing rabbit corneal epithelial wounds: immunofluorescence and ultrastructural studies. *J. Cell Biol.* **98**, 128–138.
- Colvin, R. B. (1989) Fibronectin in wound healing. In *Fibronectin*, (Ed. Mosher, D. F.). Pp. 213–254. Academic Press Inc., San Diego.
- Couchman, J. R., Austria, M. R. and Woods, A. (1990) Fibronectin-cell interactions. *J. Invest. Dermatol.* **94**, 7S–14S.
- Clark, R. A. F. (1990) Fibronectin matrix deposition and fibronectin receptor expression in healing and normal skin. *J. Invest. Dermatol.* **94**, 128S–134S.
- Welch, M. P., Odland, G. F. and Clark, R. A. F. (1990) Temporal relationships of F-actin bundle formation, collagen and fibronectin matrix assembly, and fibronectin receptor expression to wound contraction. *J. Cell Biol.* **110**, 133–145.
- Scott, J. E. (1988) Proteoglycan-fibrillar collagen interactions. *Biochem. J.* **252**, 313–323.
- Funderburgh, J. L., Cintron, C., Covington, H. I. and Conrad, G. W. (1988) Immunoanalysis of keratan sulfate proteoglycan from corneal scars. *Invest. Ophthalmol. Vis. Sci.* **29**, 1116–1124.
- Hassell, J. R., Cintron, C., Kublin, C. and Newsome, D. A. (1983) Proteoglycan changes during restoration of transparency in corneal scars. *Arch. Biochem. Biophys.* **222**, 362–369.
- Funderburgh, J. L. and Chandler, J. W. (1989) Proteoglycans of rabbit corneas with nonpenetrating wounds. *Invest. Ophthalmol. Vis. Sci.* **30**, 435–442.
- Newsome, D. A., Gross, J. and Hassell, J. R. (1982) Human corneal stroma contains three distinct collagens. *Invest. Ophthalmol. Vis. Sci.* **22**, 376–381.
- Marshall, G. E., Konstas, A. G. and Lee, W. R. (1991) Immunogold fine structural localization of extracellular matrix components in aged human cornea. I. Types I–IV collagen and laminin. *Graefes Arch. Klin. Exp. Ophthalmol.* **229**, 157–163.
- Nakayasu, K., Tanaka, M., Konomi, H. and Hayashi, T. (1986) Distribution of types I, II, III, IV and V collagen in normal and keratoconus corneas. *Ophthalmic Res.* **8**, 1–10.
- Schmut, O. (1977) The identification of type III collagen in calf and bovine cornea and sclera. *Exp. Eye Res.* **25**, 505–509.
- Praus, R., Brettschneider, I. and Adam, M. (1979) Heterogeneity of the bovine corneal collagen. *Exp. Eye Res.* **29**, 469–477.
- Cintron, C., Hong, B. S., Covington, H. I. and Macarak, E. J. (1988) Heterogeneity of collagens in rabbit cornea: type III collagen. *Invest. Ophthalmol. Vis. Sci.* **29**, 767–775.
- Tseng, S. C. G., Smuckler, D. and Stern, R. (1982) Comparison of collagen types in adult and fetal bovine corneas. *J. Biol. Chem.* **257**, 2627–2633.
- Lee, R. E. and Davison, P. F. (1984) The collagens of the developing bovine cornea. *Exp. Eye Res.* **39**, 639–652.

26. Fleischmajer, R., Perlish, J. S., Burgeson, R. E., Shaikh-Bahai, F. and Timpl, R. (1990) Type I and type III interactions during fibrillogenesis. *Ann. New York Acad. Sci.* **580**, 161–175.
27. Cho, H., Covington, H. I. and Cintron, C. (1990) Immunolocalization of type VI collagen in developing and healing rabbit cornea. *Invest. Ophthalmol. Vis. Sci.* **31**, 1096–1102.
28. Zimmermann, D. R., Trueb, B., Winterhalter, K. H., Witmer, R. and Fischer, R. W. (1986) Type VI collagen is a major component of the human cornea. *FEBS Letters* **197**, 55–58.
29. Murata, Y., Yoshioka, H., Kitaoka, M., Iyama, K., Okomura, R. and Osuku, G. (1990) Type VI collagen in healing rabbit corneal wounds. *Ophthalmic Res.* **22**, 144–151.
30. Chu, M. L., Pan, T. C., Conway, D., Saitta, B., Stokes, D., Kuo, H.-J., Glanville, R. W., Timpl, R., Mann, K. and Deutzmann, R. (1990) The structure of type VI collagen. *Ann. New York Acad. Sci.* **580**, 32–43.
31. Marshall, G. E., Konstas, A. G. and Lee, W. R. (1991) Immunogold fine structural localization of extracellular matrix components in aged human cornea. II. Collagen types V and VI. *Graefes Arch. Klin. Exp. Ophthalmol.* **229**, 164–171.
32. Gipson, I. K., Spurr-Michaud, S. J. and Tisdale, A. S. (1987) Anchoring fibrils form a complex network in human and rabbit cornea. *Invest. Ophthalmol. Vis. Sci.* **28**, 212–220.
33. Burgeson, R. E., Lunstrum, G. P., Rokosova, B., Rinberg, C. S., Rosenbaum, L. M. and Keene, D. R. (1990) The structure and function of type VII collagen. *Ann. New York Acad. Sci.* **580**, 32–43.
34. Stock, E. L., Kurpakus, M. A., Sambol, B. and Jones, J. C. (1992) Adhesion complex formation after small keratectomy wounds in the cornea. *Invest. Ophthalmol. Vis. Sci.* **33**, 304–313.
35. Gipson, I. K., Spurr-Michaud, S., Tisdale, A. and Keough, M. (1989) Reassembly of the anchoring structures of the corneal epithelium during wound repair in the rabbit. *Invest. Ophthalmol. Vis. Sci.* **30**, 425–434.
36. SundarRaj, N., Anderson, S. and Barbacci-Tobin, E. (1988) An intermediate filament-associated developmentally regulated protein in corneal fibroblasts. *Curr. Eye Res.* **7**, 939–945.
37. SundarRaj, N., Wilson, J., Gregory, J. D. and Damle, S. P. (1984) Monoclonal antibodies to proteokeratan sulfate of rabbit corneal stroma. *Curr. Eye Res.* **4**, 49–54.
38. SundarRaj, N., Martin, J. and Hrinya, N. (1982) Development and characterization of monoclonal antibodies to human type III procollagen. *Biochem. Biophys. Res. Commun.* **106**, 48–57.
39. Kurpakus, M. A., Stock, E. L. and Jones, J. C. R. (1990) Analysis of wound healing in an *in vitro* model: early appearance of laminin and a $125 \times 10^3 M_r$ polypeptide during adhesion complex formation. *J. Cell Sci.* **96**, 651–660.
40. Garana, R. M. R., Petroll, W. M., Chen, W. T., Herman, I. B., Barry, P., Andrews, P., Covanaugh, H. D. and Jester, J. V. (1992) Radial keratotomy. II. Role of the myofibroblast in corneal wound contraction. *Invest. Ophthalmol. Vis. Sci.* **33**, 3271–3282.
41. Cintron, C., Covington, H. I. and Kublin, C. L. (1990) Morphologic analyses of proteoglycans in rabbit corneal scars. *Invest. Ophthalmol. Vis. Sci.* **31**, 1789–1798.
42. Scott, J. E. and Haigh, M. (1988) Keratan sulphate and the ultrastructure of cornea and cartilage: a 'stand-in' for chondroitin sulphate in conditions of oxygen lack? *J. Anat.* **158**, 95–108.
43. Melles, G. R. J., SundarRaj, N., Binder, P. S., Weiden, M. M., Wijdh, R. H. J., Beekhuis, W. H., Moo, C. M. and Anderson, J. A. (1993) Epithelial-stromal interactions in unsutured and sutured wounds within the same monkey cornea. (Abstract) *Invest. Ophthalmol. Vis. Sci.* **34** (Suppl), 2184.
44. Melles, G. R. J., Binder, P. S. and Anderson, J. A. (1994) Variation in healing throughout the depth of long-term, unsutured, corneal wounds in human autopsy specimens and monkeys. *Arch. Ophthalmol.* **112**, 100–109.